Evaluation of efficacy- versus affinity-driven agonism with biased GLP-1R ligands P5 and exendin-F1

Marzook, Amaara; Chen, Shiqian; Pickford, Philip; Lucey, Maria A.; Wang, Yifan; Corrêa, Ivan R; Broichhagen, Johannes; Hodson, David; Salem, Victoria; Rutter, Guy A; Tan, Tricia M.; Bloom, Stephen R.; Tomas, Alejandra; Jones, Ben

DOI:
10.1016/j.bcp.2021.114656

Biochemical Pharmacology 190 (2021) 114656

Contents lists available at ScienceDirect

Biochemical Pharmacology

journal homepage: www.elsevier.com/locate/biochempharm

Evaluation of efficacy- *versus* affinity-driven agonism with biased GLP-1R ligands P5 and exendin-F1

Amaara Marzook [a], Shiqian Chen [a], Phil Pickford [a], Maria Lucey [a], Yifan Wang [b], Ivan R. Corrêa Jr [c], Johannes Broichhagen [d], David J. Hodson [e,f,g], Victoria Salem [a,h], Guy A. Rutter [b,i], Tricia M. Tan [a], Stephen R. Bloom [a], Alejandra Tomas [b,*], Ben Jones [a,*]

[a] Section of Endocrinology and Investigative Medicine, Imperial College London, London, United Kingdom
[b] Section of Cell Biology and Functional Genomics, Imperial College London, London, United Kingdom
[c] New England Biolabs, Ipswich, MA, USA
[d] Leibniz-Forschungsinstitut für Molekulare Pharmakologie, Berlin, Germany
[e] Institute of Metabolism and Systems Research (IMSR), University of Birmingham, Birmingham, United Kingdom
[f] Centre for Endocrinology, Diabetes and Metabolism, Birmingham Health Partners, Birmingham, United Kingdom
[g] Centre of Membrane Proteins and Receptors (COMPARE), Universities of Birmingham and Nottingham, Midlands, United Kingdom
[h] Department of Bioengineering, Imperial College London, London, United Kingdom
[i] Lee Kong Chian School of Medicine, Nanyang Technological University, Singapore

ARTICLE INFO

Keywords:
GLP-1R
Biased agonism
Endocytosis
Exendin-4
β-arrestin

ABSTRACT

The glucagon-like peptide-1 receptor (GLP-1R) is an important regulator of glucose homeostasis and has been successfully targeted for the treatment of type 2 diabetes. Recently described biased GLP-1R agonists with selective reductions in β-arrestin *versus* G protein coupling show improved metabolic actions *in vivo*. However, two prototypical G protein-favouring GLP-1R agonists, P5 and exendin-F1, are reported to show divergent effects on insulin secretion. In this study we aimed to resolve this discrepancy by performing a side-by-side characterisation of these two ligands across a variety of *in vitro* and *in vivo* assays. Exendin-F1 showed reduced acute efficacy *versus* P5 for several readouts, including recruitment of mini-G proteins, G protein-coupled receptor kinases (GRKs) and β-arrestin-2. Maximal responses were also lower for both GLP-1R internalisation and the presence of active GLP-1R-mini-G_s complexes in early endosomes with exendin-F1 treatment. In contrast, prolonged insulin secretion *in vitro* and sustained anti-hyperglycaemic efficacy in mice were both greater with exendin-F1 than with P5. We conclude that the particularly low acute efficacy of exendin-F1 and associated reductions in GLP-1R downregulation appear to be more important than preservation of endosomal signalling to allow sustained insulin secretion responses. This has implications for the ongoing development of affinity- *versus* efficacy-driven biased GLP-1R agonists as treatments for metabolic disease.

1. Introduction

With the increasing worldwide prevalence of type 2 diabetes (T2D) [1], there is an urgent need for more effective drugs to treat this condition. T2D results from a combination of relative insulin deficiency and resistance to its action in central and peripheral tissues, and is commonly associated with excess adiposity or obesity [2]. The glucagon-like peptide-1 receptor (GLP-1R), a class B G protein-coupled receptor (GPCR) expressed at high levels in pancreatic beta cells and at lower levels in anorectic centres in the brain, is a well-established target for pharmacological T2D treatment [3]. GLP-1R activation augments glucose-stimulated insulin secretion, improves beta cell survival and suppresses appetite, with the latter resulting in weight loss and improvements in insulin sensitivity [4]. Pharmacokinetically optimised GLP-1R agonists based on the amino acid sequence of either the cognate agonist GLP-1(7–36)NH_2 or its homologue exendin-4 [5] are approved for the treatment of T2D. These agents not only improve glycaemic control and induce weight loss but also reduce cardiovascular [6] and all-cause mortality [7] in people with T2D.

Recent preclinical studies have shown that GLP-1R agonists that

* Corresponding authors at: Section of Endocrinology and Investigative Medicine, Imperial College London, London, W12 0NN, United Kingdom (B. Jones). Section of Cell Biology and Functional Genomics, Imperial College London, London, W12 0NN, United Kingdom (A. Tomas).

https://doi.org/10.1016/j.bcp.2021.114656
Received 22 March 2021; Received in revised form 9 June 2021; Accepted 11 June 2021
Available online 12 June 2021

favour G protein signalling and generation of cyclic adenosine monophosphate (cAMP) over β-arrestin recruitment are particularly effective at reducing blood glucose levels [8–12]. Moreover, it is suggested that the markedly reduced β-arrestin recruitment seen at the GLP-1R with the dual GLP-1R/glucose-dependent insulinotropic peptide receptor (GIPR) agonist Tirzepatide [13–15] may contribute to its superior anti-diabetic efficacy in clinical trials [16]. An appealing explanation for the effects of these "biased" GLP-1R agonists is that reductions in β-arrestin-mediated desensitisation, as well as a trafficking phenotype that favours preservation of GLP-1R at the plasma membrane, lead to prolonged intracellular signalling and cumulatively greater insulin release over time. However, this has not been demonstrated for all published examples of biased GLP-1R agonists. In particular, "P5", the first bespoke biased GLP-1R agonist to be described, was potently anti-hyperglycaemic but poorly insulinotropic *in vivo*, with its metabolic effects instead partly attributed to increases in adipogenesis [8]. This contrasts with "exendin-phe1" [9] (referred to here as "exendin-F1"), a peptide that showed marked increases in insulin release compared to exendin-4 in cellular models and in mice. One possible explanation for this discrepancy is that different approaches were used to evaluate the two ligands, with exendin-F1 tested using prolonged incubations with beta cells and islets, as well as sub-chronic *in vivo* studies, to specifically seek functional evidence of reduced desensitisation over the course of several hours [9]. However, to date, P5 has not been examined in this way.

Establishing a consensus mechanism of action for biased GLP-1R agonists would help guide their development for the treatment of T2D and related metabolic diseases. In the present work we perform direct pharmacological comparisons of P5 and exendin-F1, with exendin-4 included as the reference peptide. As well as determining relative preferences for G protein and β-arrestin recruitment responses, we focussed in particular on differences in GLP-1R membrane trafficking and activation in different endomembrane compartments [17]. Our study highlights a number of pharmacological properties that diverge between P5 and exendin-F1, suggesting these GLP-1R agonists may in fact possess distinct modes of action.

2. Materials and methods

2.1. Peptides and other reagents

Exendin-4, exendin-F1 and P5 were all custom synthesised by Wuxi Apptec (Wuhan, China) with > 90% purity confirmed by HPLC. The synthesis of Luxendin645 and exendin-4-Cy5 have been described previously [18,19]. Unless otherwise specified, all chemicals were obtained from Sigma Aldrich (Gillingham, UK).

2.2. Cell culture

All cell culture reagents were obtained from Life Technologies (Hemel Hempstead, UK). HEK293T cells were maintained in DMEM supplemented with 10% FBS and 1% penicillin/streptomycin. HEK293-SNAP-GLP-1R cells, generated by stable transfection of pSNAP-GLP-1R (Cisbio, Codolet, France) into HEK293 cells [20], were maintained in DMEM supplemented with 10% FBS, 1% penicillin/streptomycin and 1 mg/ml G418. PathHunter CHO-K1-GLP-1R-βarr2-EA cells (DiscoverX, Fremont, USA) were maintained in Ham's F12 medium with 10% FBS and 1% penicillin/streptomycin. INS-1 832/3 cells (a gift from Prof Christopher Newgard, Duke University) [21], and subclones thereof lacking endogenous GLP-1R or GIPR after deletion by CRISPR/Cas9 (a gift from Dr Jacqueline Naylor, AstraZeneca) [22], were maintained in RPMI at 11 mM glucose, supplemented with 10% FBS, 10 mM HEPES, 1 mM pyruvate, 50 μM β-mercaptoethanol, and 1% penicillin/streptomycin.

2.3. GLP-1R competitive binding measurements

Cells were labelled with SNAP-Lumi4-Tb (Cisbio) using 40 nM probe for 60 min at 37 °C, in complete medium. After washing to remove unbound probe, cells were resuspended in HBSS with 0.1% BSA and metabolic inhibitor cocktail (20 mM 2-deoxyglucose and 10 mM NaN_3 to inhibit endocytosis, as previously described [9,23], and seeded into white opaque plates. After 20 min at room temperature, cells were then placed at 4 °C, and a range of concentrations of test ligands were applied concurrently with 10 nM Luxendin645 [19] or 5 nM exendin-4-Cy5, with a range of concentrations of Luxendin645 or exendin-4-Cy5 also applied to establish equilibrium binding parameters for the competing labelled GLP-1R probe. After a 24-hour incubation period at 4 °C, binding was measured by TR-FRET using a Spectramax i3x plate reader (Molecular Devices) fitted with an HTRF module.

2.4. NR12A conformational sensor assay

Cells were labelled with SNAP-Lumi4-Tb (40 nM, 60 min at 37 °C, in complete medium). After washing to remove unbound probe, cells were resuspended in HBSS ± 100 nM NR12A (a gift from Prof Andrey Klymchenko, University of Strasbourg) [24] for 5 min before washing again. Labelled cells were transferred to 96-well half area white plates and baseline TR-FRET signal from Lumi4-Tb (donor) and NR12A (acceptor) were recorded for 5 min at 37 °C using a Flexstation 3 plate reader with the following settings: $\lambda_{ex} = 335$ nm, $\lambda_{em} = 490$ and 590 nm, delay 50 μs, integration time 300 μs. Ligands were then added, and signal was serially monitored for 10 min. The TR-FRET ratio, i.e. the ratio of fluorescence intensities at 590 and 490 nm, was considered indicative of the proximity of the GLP-1R extracellular domain (ECD) to the plasma membrane. Baseline-normalised AUCs were used for concentration–response analysis.

2.5. cAMP assays

Resuspended cells were stimulated at 37 °C in their respective serum-free medium in 96-well half area opaque white plates before addition of HTRF lysis buffer and detection reagents (cAMP Dynamic 2 kit, Cisbio). The duration of stimulation and inclusion or not of the phosphodiesterase inhibitor 3-isobutyl-1-methylxanthine (IBMX) is indicated in the relevant figure legend. The assay was read by HTRF.

2.6. Homologous desensitisation assay in beta cells

INS-1 832/3 cells were seeded into poly-D-lysine-coated 96-well plates in complete medium at 11 mM glucose in the presence of different concentrations of test agonist. After an overnight incubation, medium was removed and cells were washed 3 times in HBSS, followed by a 1-hour resensitisation period in complete medium. Cells were then stimulated at 37 °C with 100 nM GLP-1 + 500 μM IBMX for 10 min followed by lysis and cAMP determination as described in Section 2.5.

2.7. β-arrestin-2 recruitment by enzyme complementation

PathHunter CHO-K1-GLP-1R-βarr2-EA cells were stimulated for 30 min at 37 °C in serum-free Ham's F12 medium prior to addition of lysis / detection reagents (DiscoverX). The assay was read by luminescence.

2.8. NanoBiT mini-G_s and β-arrestin-2 GLP-1R recruitment assays

These assays were performed as described previously [25]. HEK293T cells were transiently transfected using Lipofectamine 2000 (Life Technologies) with 50 ng each of GLP-1R-SmBit and LgBit-β-arrestin-2 (Promega, Southampton, UK) diluted in pcDNA3.1, or with 500 ng each of GLP-1R-SmBiT and LgBiT-mini-G_s (a gift from Prof Nevin Lambert, Medical College of Georgia) [26], per well of a 12-well plate, and the

assay was performed 24 h later. For the kinetic mode assay, cells were resuspended in HBSS containing Furimazine (Promega, 1:50), seeded into half-area opaque white plates, and total luminescent signal at baseline was recorded over 5 min at 37 °C using a Flexstation 3 plate reader. Ligands were then added, and signal was serially monitored for up to 30 min. Ligand-induced change was expressed relative to baseline values for each well. For the endpoint mode assay, cells were resuspended in HBSS and seeded into half-area opaque white plates containing prepared ligands. After a 5-minute incubation at 37 °C, Furimazine prepared in HBSS was added, and luminescent signal was recorded over 3 min using a Spectramax i3x plate reader.

2.9. NanoBRET GLP-1R recruitment assays

GRK2-Venus, GRK5-Venus and GRK6-Venus were gifts from Prof Denise Wootten, Monash University. Nb37-GFP [27] was a gift from Dr Roshanak Irannejad, University of California, San Francisco. HEK293T cells were transfected using Lipofectamine 2000 with 50 ng of plasmid encoding SNAP-GLP-1R with a C-terminal nanoluciferase tag (SNAP-GLP-1R-Nluc) and 50 ng of fluorescent protein BRET acceptor plasmid per well of a 12-well plate, diluted with pcDNA3.1, and the assay was performed 24 h later. SNAP-GLP-1R-Nluc was generated in *house* by PCR cloning of the nanoluciferase sequence from pcDNA3.1-ccdB-Nanoluc (a gift from Mikko Taipale; Addgene plasmid # 87067) onto the C-terminus end of the SNAP-GLP-1R vector (Cisbio), followed by site-directed mutagenesis of the GLP-1R stop codon. Cells were resuspended in HBSS containing Furimazine (1:50), seeded into 96-well half-area opaque white plates, and baseline luminescent signals recorded at 460 nm (Nluc emission peak) and 520 nm (GFP acceptor peak) or 535 nm (Venus acceptor peak) over 5 min at 37 °C using a Flexstation 3 plate reader. Ligands were added, and signal was serially monitored for up to 20 min. Signal was expressed ratiometrically for each time-point as GFP or Venus acceptor divided by Nluc donor signal. The BRET ratio at each time-point was first expressed relative to the average baseline value for each well, followed by subtraction of the vehicle signal at each time-point to provide net BRET.

2.10. NanoBRET bystander assays

HEK293-SNAP-GLP-1R cells were transiently transfected using Lipofectamine 2000 with 50 ng of mini-G_s-Nluc or β-arrestin-2-CyOFP [28] plus 50 ng of KRAS-Venus or Rab5-Venus (all gifts from Prof Nevin Lambert, Medical College of Georgia) per well of a 12-well plate, diluted with pcDNA3.1, and the assay was performed 24 h later as described in Section 2.9.

2.11. DERET assay

The assay was performed as described previously [25]. Cells were labelled with SNAP-Lumi4-Tb (40 nM, 60 min at 37 °C, in complete medium). After washing, labelled cells were resuspended in HBSS containing 24 μM fluorescein. TR-FRET signals at baseline and serially after agonist addition were recorded at 37 °C using a Flexstation 3 plate reader using the following settings: λ_{ex} = 335 nm, λ_{em} = 520 and 620 nm, delay 400 μs, integration time 1500 μs. Receptor internalisation was quantified as the ratio of fluorescent signal at 620 nm to that at 520 nm, after subtraction of individual wavelength signals obtained from wells containing 24 μM fluorescein only.

2.12. LysoTracker TR-FRET internalisation assay

Cells were labelled with SNAP-Lumi4-Tb (40 nM, 60 min at 37 °C, in complete medium), with 100 nM LysoTracker Red DND99 (Life Technologies) added for the last 15 min of the incubation. After washing, labelled cells were resuspended in HBSS. TR-FRET signals at baseline and serially after agonist addition were recorded at 37 °C using a Flexstation 3 plate reader using the following settings: λ_{ex} = 335 nm, λ_{em} = 550 and 610 nm, delay 50 μs, integration time 300 μs. Receptor translocation to acidic endosomes was quantified as the ratio of fluorescent signal at 610 nm to that at 550 nm.

2.13. GLP-1R clustering assay

The assay was performed as previously described [20]. Cells were dual labelled with SNAP-Lumi4-Tb (40 nM) and 500 nM SNAP-Surface-649 (New England Biolabs, Hitchin, UK) for 30 min at 37 °C, in complete medium. After washing, labelled cells were resuspended in HBSS. TR-FRET signals at baseline and serially after agonist addition were recorded at 37 °C using a Spectramax i3x plate reader with HTRF module. GLP-1R clustering was quantified as the ratio of the fluorescence signal at 665 nm to that at 616 nm.

2.14. Visualisation of GLP-1R subcellular localisation

Cells were seeded onto glass coverslips and labelled with SNAP-Surface-549 (1 μM, 30 min, 37 °C). After agonist stimulation and paraformaldehyde fixation, coverslips were mounted onto glass slides using Diamond Prolong antifade with DAPI (Life Technologies). Slides were imaged using a Nikon Ti2E microscope frame with integrated hardware from Cairn Research (Faversham, UK) incorporating motorised stage (ASI), LED illumination source (CoolLED) and a 100X oil immersion objective. Z-stacks were acquired and deconvolved using Deconvolutionlab2 [29] using the Richardson Lucy algorithm. Images were processed in Fiji.

2.15. High content microscopy trafficking assay

The assay was performed as previously described [25]. Cells were seeded into poly-D-lysine-coated, black 96-well plates. On the day of the assay, cells were labelled with BG-S-S-649 (1 μM, a gift from New England Biolabs). After washing, agonists were applied for 30 min at 37 °C in complete medium. Agonists were removed, cells washed with cold HBSS and then placed on ice for subsequent steps. Mesna (100 mM in alkaline TNE buffer, pH 8.6) or alkaline TNE without Mesna was applied for 5 min, and then washed with HBSS. Microplates were then imaged using the microscope system described in Section 2.14 fitted with a 20X phase contrast objective, with data acquisition controlled by the openHCA software written for the MicroManager platform [30]. 9 random images per well were acquired for both epifluorescence and transmitted phase contrast. HBSS was then removed and replaced with fresh complete medium. Receptor was allowed to recycle for 60 min at 37 °C, followed by a second Mesna application to remove any receptor that had recycled to the membrane, and the plate was re-imaged as above. Internalised SNAP-GLP-1R was quantified at both time points using Fiji as follows: 1) phase contrast images were processed using PHANTAST [31] to segment cell-containing regions from background; 2) illumination correction of fluorescence images was performed using BaSiC [32]; 3) fluorescence intensity was quantified for cell-containing regions. Agonist-mediated internalisation was determined as the mean signal for each condition normalised to signal from wells not treated with Mesna, after first subtracting non-specific fluorescence determined from wells treated with Mesna but no agonist. The percentage of reduction in residual internalised receptor after the second Mesna treatment was considered to represent recycled receptor. Recycling was then expressed as a percentage relative to the amount of receptor originally internalised in the same well.

2.16. Overnight stimulation surface labelling assay

INS-1-SNAP-GLP-1R cells were seeded into poly-D-lysine-coated, black 96-well plates with agonists applied in complete medium at 11 mM glucose. After an overnight incubation, agonists were removed, and

cells washed with HBSS. Cells were then labelled with BG-S-S-649 (1 μM in complete medium, 30 min) before washing and imaging as in Section 2.15. Surface labelling intensity was quantified as in Section 2.15 with subtraction of signal from INS to 1 832/3 cells without SNAP-GLP-1R but labelled with BG-S-S-649.

2.17. Insulin secretion assay

After a prior 6 h at 3 mM glucose, INS-1 832/3 cells were seeded overnight in 96-well plates in complete medium at 11 mM glucose ± test agonists. A sample of supernatant was removed and analysed for insulin content by HTRF (Wide Range Insulin HTRF Kit, Cisbio). Results were expressed relative to insulin released with 11 mM glucose alone.

2.18. In vivo study

Animals were maintained in specific pathogen-free facilities, with *ad lib* access to food (except prior to fasting studies) and water. Studies were regulated by the UK Animals (Scientific Procedures) Act 1986 of the U.K. and approved by Imperial College London (Project License PB7CFFE7A). Male C57Bl/6 mice (8–10 weeks of age, weight 25–30 g, supplied by Charles River, UK) were injected intra-peritoneally (IP) during the light phase with 2.4 nmol/kg agonist prepared in 100 μl 0.9% NaCl, or vehicle. Food was removed from the cages at this point until the end of the study. After an 8-hour delay, mice were injected IP with 20% dextrose (2 g/kg). Blood glucose levels were monitored immediately before glucose administration and at 20-min intervals thereafter from tail vein blood samples using a hand-held glucose meter.

2.19. Data analysis

All analyses were performed using Prism 8 (GraphPad Software). The average of within-assay replicates was counted as one biological replicate. For equilibrium binding studies, Luxendin645 and exendin-4-Cy5 K_d values were fitted using a "one site – specific binding" model. Test ligand K_i values were determined using a "one site – fit K_i" model. Functional concentration response data were fitted using 3-parameter logistic fitting, with constraints applied where appropriate. Bias analysis was performed by the calculation of transduction coefficients (i.e. τ/K_A values) as previously described [9,33,34], with subtraction of the $\text{Log}(\tau/K_A)$ value for one pathway (cAMP or mini-G_s) from the second pathway (β-arrestin-2) to give $\Delta\text{Log}(\tau/K_A)$. The assays for which bias was calculated were performed with both pathways assessed in parallel using the same ligand stock, allowing statistical comparisons on a per-assay basis. In the instances when a composite parameter was determined from two assay types not performed in parallel (i.e. the pEC_{50} -

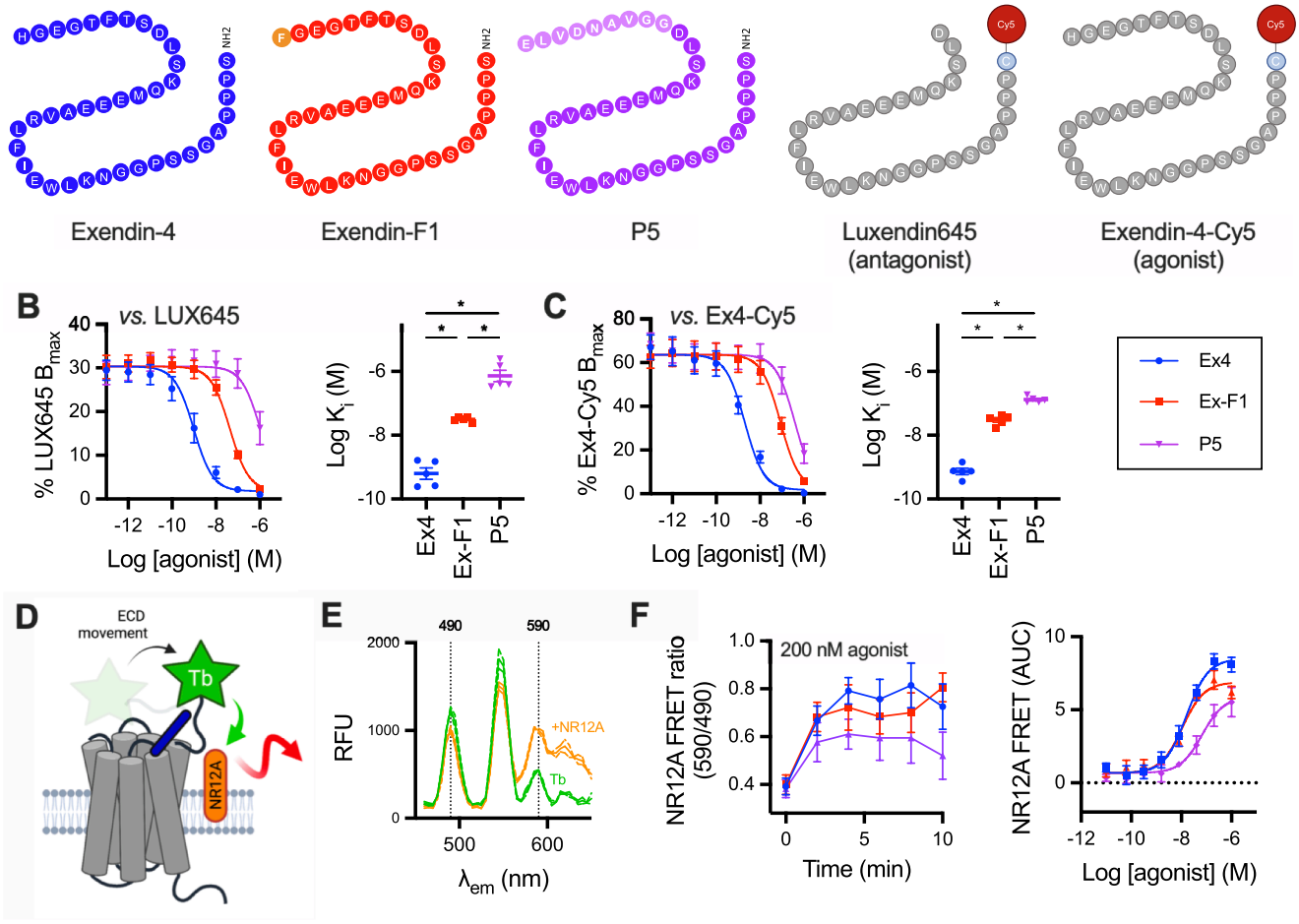

Fig. 1. Ligand-receptor binding and conformational rearrangement with GLP-1R agonists. (**A**) Schematic showing amino acid sequences of peptide ligands used in this study in single letter code. (**B**) Competitive binding of each ligand in competition with 10 nM Luxendin645 (LUX645), $n = 5$, with calculated K_i shown and compared by one-way randomised block ANOVA with Tukey's test. (**C**) As for (B) but with 5 nM exendin-4-Cy5 (Ex4-Cy5) as the competing ligand, $n = 5$. (**D**) Principle of NR12A assay (cartoon generated using Biorender), showing how ligand-induced Lumi4-Tb-labelled SNAP-GLP-1R ECD movement leads to an increase in energy transfer to the plasma membrane probe NR12A, detected as an increase in TR-FRET. (**E**) The TR-FRET spectrum of Lumi4-Tb-labelled HEK293-SNAP-GLP-1R cells with and without co-labelling with 100 nM NR12A, $n = 2$. (**F**) ECD movement response with NR12A + Lumi4-Tb-labelled HEK293-SNAP-GLP-1R cells stimulated with exendin-4, exendin-F1 or P5, $n = 4$. Kinetic and concentration responses are displayed. * $p < 0.05$ by indicated statistical test. Data are represented as mean ± SEM, with individual replicates shown where possible.

pK_i measurement in Fig. 1), error propagation was performed. Statistical comparisons were performed by *t*-test, one-way ANOVA or two-way ANOVA as appropriate. Paired or matched analyses were performed where permitted by the experimental design. Specific post-hoc tests are indicated in the legends. Statistical significance was assigned if $p < 0.05$. Data are represented as mean ± standard error of the mean (SEM) throughout, with individual replicates indicated where possible.

3. Results

3.1. Contrasting efficacy and affinity with P5 versus exendin-F1.

We first measured the equilibrium binding affinities of exendin-4, exendin-F1 and P5 (Fig. 1A) in HEK293 cells stably expressing SNAP-GLP-1R [35], using a competitive time-resolved FRET (TR-FRET) assay in which the receptor N-terminus is labelled with the energy donor Lumi4-Tb to detect binding of Cy5-conjugated GLP-1R antagonist exendin(9–39) ("Luxendin645") [19] or the equivalent agonist, exendin-4-Cy5 [18], applied in competition with unlabelled test peptides (Fig. 1B and 1C, Table 1). Both G protein-biased ligands displayed significantly lower affinity for receptor binding than exendin-4; of note, the K_i for P5 was 22-fold higher than for exendin-F1 when measured using Luxendin645 as the competing probe but only 4-fold higher with exendin-4-Cy5. As an additional measure of ligand-receptor interaction, we also established a TR-FRET approach to monitor movements between the GLP-1R SNAP-tagged extracellular domain (ECD) and the plasma membrane, labelled using the membrane probe NR12A [24], as recently applied for the GLP-1R using the related probe NR12S [36] and by microscopy for the epidermal growth factor receptor (EGFR) [37]. GLP-1R in its inactive state adopts a "closed" conformation, in which the ECD is apposed to the extracellular loops [38], from which it is released on ligand binding [39]. In our assay, agonist-induced conformational change brings the ECD closer to the plasma membrane, causing an increase in FRET signal between Lumi4-Tb and NR12A (Fig. 1D, 1E). Interestingly, across a full concentration range, exendin-F1 showed similar potency to exendin-4, with a non-significantly lower efficacy, whereas P5 potency and efficacy were both lower (Fig. 1F, Table 1).

Having established differences in binding parameters and ability to induce GLP-1R conformational shifts, we aimed to establish differences in intracellular signalling and transducer coupling. Measurement of cAMP production in HEK293-SNAP-GLP-1R cells showed reduced potency for both exendin-F1 and P5 (Fig. 2A, Table 1), but the differences between agonists were smaller than for equilibrium binding affinity in the same cell model, suggesting ligand-specific differences in coupling of receptor occupancy to cAMP production (Fig. 2B). This observation has been made before for P5 [40] and exendin-F1 [35], but here the ligands are compared directly for the first time.

Balance between G protein pathway engagement and β-arrestin-2 recruitment was assessed using two approaches. Firstly, using the PathHunter system [9], cAMP production and β-arrestin-2 recruitment were measured in parallel, which highlighted how exendin-F1 and P5 show low efficacy as well as reduced potency for β-arrestin-2 (Fig. 2C, Table 1). β-arrestin-2 recruitment efficacy was greater for P5 than for exendin-F1. Comparison of transduction ratios (τ/K_A) determined using the operational model for each pathway [34] indicated a substantial degree of bias in favour of cAMP production for both P5 and exendin-F1, with the effect being most marked for the latter (~60-fold *versus* 15-fold). Secondly, recruitment of mini-G_s and β-arrestin-2 to GLP-1R were measured by nanoBiT complementation [26,41], with response kinetics shown in Fig. 2D and concentration-responses at 5 min in Fig. 2E (see also Table 1). These analyses confirmed low efficacy β-arrestin-2 recruitment but also reduced recruitment efficacy for mini-G_s with exendin-F1 and P5. Maximum responses with exendin-F1 were reduced in comparison to P5 in both pathways, to the extent that the β-arrestin-2 response was not amenable to logistic curve fitting for the former ligand. Interestingly, no significant bias could be detected for P5 *versus* exendin-4 from these data; bias for exendin-F1 could not be determined due to the lack of a quantifiable β-arrestin-2 response.

We also investigated the relative propensity for each ligand to recruit G protein-coupled receptor kinases (GRKs) to the GLP-1R, an intermediate step that typically precedes recruitment of β-arrestins to GPCRs, including GLP-1R [42,43]. Even at a high (100 nM) stimulatory concentration, exendin-F1 showed very minimal recruitment of GRK2 to GLP-1R compared to exendin-4, as measured by BRET between SNAP-GLP-1R tagged at the C-terminus with nanoluciferase (SNAP-GLP-1R-Nluc) and GRK2-Venus, with an intermediate effect for P5 (Fig. 2F). Ligand-induced changes were barely detectable for GRK5 and 6.

We also designed a BRET-based sensor strategy to monitor differences in ligand-induced activation (as opposed to recruitment) of endogenous G proteins by co-expressing SNAP-GLP-1R-Nluc with GFP-tagged nanobody-37 (Nb37), a genetically encoded intrabody that recognises the active conformation of $G\alpha_S$ [27]. Interestingly, the Nb37 response to exendin-F1, but not P5, was reduced in comparison to exendin-4 in HEK293 cells (Fig. 2G). The low dynamic range of this sensor configuration precluded concentration–response analyses.

Overall, these data highlight how exendin-F1 has a higher GLP-1R binding affinity than P5 but lower efficacy for recruitment of mini-G_s, GRK2 and β-arrestin-2, as well as reduced $G\alpha_s$ activation, which implies greater coupling efficiency of GLP-1R occupancy to intracellular responses with P5 *versus* exendin-F1. However, the higher affinity of exendin-F1 results in comparable acute cAMP signalling responses between both biased agonists in the heterologous cell system used for these studies.

3.2. GLP-1R trafficking with exendin-F1 and P5

An altered membrane trafficking profile characterised by reduced

Table 1
Parameter estimates for pharmacological responses to GLP-1R agonists. Mean ± SEM for 3-parameter fit-derived potency and efficacy estimates from Figs. 1, 2 and 3. For E_{max}, where all ligands were full agonists, values are normalised to a "global" E_{max} obtained for each assay, whereas where only exendin-4 was a full agonist, exendin-F1 and P5 E_{max} values are expressed relative to exendin-4. Statistical comparisons are by one-way randomised block ANOVA with Tukey's test. Statistical testing for E_{max} values was performed on data prior to normalisation. * $p < 0.05$ *versus* exendin-4; # $p < 0.05$ exendin-F1 *versus* P5. n.c. = not calculable.

	Exendin-4		Exendin-F1		P5	
Assay and cell model	pEC_{50} (M)	E_{max} (%)	pEC_{50} (M)	E_{max} (%)	pEC_{50} (M)	E_{max} (%)
ECD conformational sensor (HEK293-SNAP-GLP-1R)	7.8 ± 0.1	8.5 ± 0.3	8.0 ± 0.1	6.9 ± 0.4	7.2 ± 0.2 *,#	6.1 ± 0.9 *
cAMP (HEK293-SNAP-GLP-1R)	9.9 ± 0.1	95 ± 5	8.7 ± 0.1 *	98 ± 6	8.4 ± 0.1 *,#	92 ± 5
cAMP (PathHunter)	10.3 ± 0.1	97 ± 1	9.4 ± 0.1 *	105 ± 3	9.3 ± 0.1 *	107 ± 2 *
β-arrestin2 (PathHunter)	7.5 ± 0.2	100	6.4 ± 0.2 *	15 ± 0 *	6.3 ± 0 *	36 ± 3 *,#
NanoBiT mini-G_s (HEK293T)	7.7 ± 0.1	100	7.1 ± 0.3	10 ± 2 *	7.1 ± 0.1	38 ± 7 *
NanoBiT β-arrestin2 (HEK293T)	7.4 ± 0.1	100	n.c.	n.c.	6.8 ± 0.2 *	46 ± 7 *
Internalisation by microscopy (HEK293-SNAP-GLP-1R)	8.3 ± 0.1	93 ± 8	7.2 ± 0.1 *	17 ± 4 *	6.8 ± 0.2 *	64 ± 5 *,#
Internalisation by DERET (HEK293-SNAP-GLP-1R)	8.5 ± 0.2	100	n.c.	n.c.	n.c.	n.c.
Lysosomal redistribution (HEK293-SNAP-GLP-1R)	8.0 ± 0.2	100	n.c.	n.c.	n.c.	n.c.

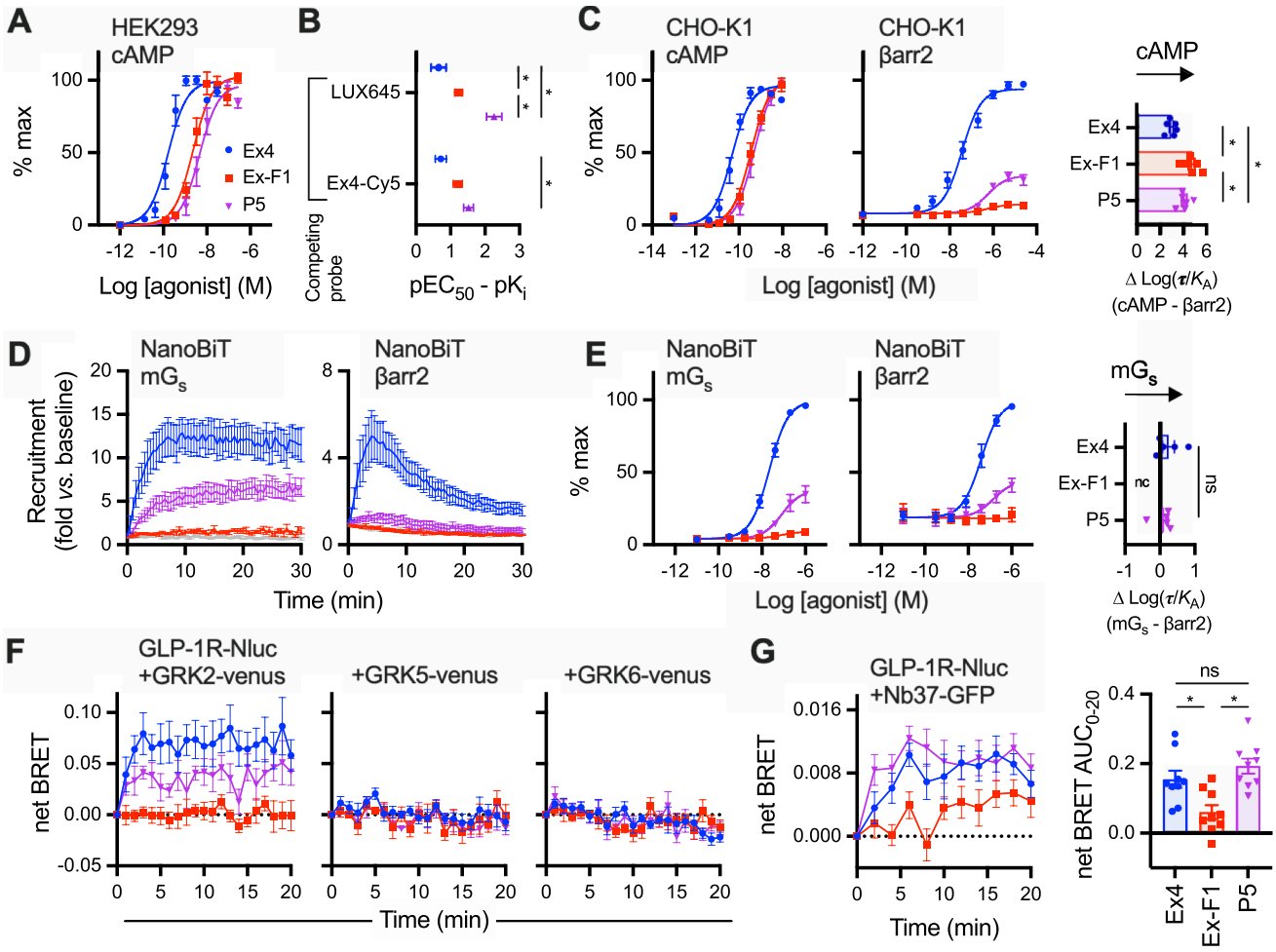

Fig. 2. Signalling and transducer coupling. (**A**) cAMP production in HEK293-SNAP-GLP-1R cells, 30-min stimulation, normalised to global maximum response, with 3-parameter fit shown, $n = 5$. (**B**) cAMP potency from (A) expressed relative to affinity from Fig. 1, with error propagation, and comparison by two-way ANOVA with Tukey's test. (**C**) cAMP production and recruitment of β-arrestin-2 (βarr2) in PathHunter CHO-K1-βarr2-EA cells, 30-min stimulation, normalised to full agonist global maximum response, with 3-parameter fit, $n = 6$, and bias determination as $\Delta\text{Log}(\tau/K_A)$ (cAMP *versus* β-arrestin-2 for each ligand) shown and compared by one-way randomised block ANOVA with Tukey's test. (**D**) 100 nM ligand-induced recruitment of mini-G_s (mG_s) and β-arrestin-2 to GLP-1R, measured by nanoBiT complementation in transiently transfected HEK293 cells, $n = 5$. (**E**) Ligand-induced recruitment of mini-G_s (mG_s) and β-arrestin-2 to GLP-1R at 5 min, measured by nanoBiT complementation in transiently transfected HEK293 cells, $n = 5$, with bias determination as $\Delta\text{Log}(\tau/K_A)$ shown and compared by paired *t*-test (exendin-4 *versus* P5). (**F**) Recruitment of GRK2-Venus, GRK5-Venus, or GRK6-Venus to GLP-1R-Nluc in transiently transfected HEK293T cells, with 100 nM agonist applied, all $n = 6$. (**G**) Recruitment of Nb37-GFP to GLP-1R in response to 100 nM agonist in HEK293T cells, $n = 9$, with AUC shown and compared by one-way randomised block ANOVA with Tukey's test. * $p < 0.05$ by indicated statistical test. Data are represented as mean ± SEM, with individual replicates shown where possible.

endocytosis and faster recycling is thought to be an important component of the action of biased GLP-1R agonists such as exendin-F1 [9], but has not been tested for P5. Using high content microscopy [25], we confirmed that both exendin-F1 and P5 showed reduced GLP-1R internalisation propensity but faster recycling than exendin-4 (Fig. 3A, Table 1). The reduction in efficacy was again most pronounced with exendin-F1 but potency was slightly lower with P5; relative potencies for each ligand *versus* exendin-4 were in line with those for cAMP production in the same cell model. Higher resolution images of GLP-1R subcellular localisation with each ligand are shown in Fig. 3B, revealing that a substantial proportion of GLP-1R remains at the plasma membrane after stimulation with both biased GLP-1R agonists, in comparison to exendin-4. Kinetics of GLP-1R internalisation were assessed by diffusion-enhanced resonance energy transfer (DERET) [44], with very little response detected with either exendin-F1 or P5 below 100 nM (Fig. 3C, Table 1).

We also developed a time-resolved FRET (TR-FRET) assay to monitor translocation of lanthanide-labelled SNAP-GLP-1R to the late endolysosomal compartment, which was labelled using the chemical endolysomotropic dye LysoTracker DND99. This highlighted how exendin-4 rapidly targets internalised GLP-1Rs towards this degradative compartment (Fig. 3D, Table 1). In these studies, performed in parallel to DERET measurements, the EC_{50} for exendin-4-induced GLP-1R lysosomal localisation was somewhat higher than for internalisation *per se*, implying that not all internalised GLP-1Rs are targeted to the lysosome.

As spatial reorganisation of activated GLP-1Rs into tightly constrained nanodomains precedes endocytosis [20], we also compared GLP-1R clustering with each ligand using a dual-labelling TR-FRET assay. GLP-1R clustering was barely detectable at 100 nM agonist with exendin-F1 or P5, but exendin-4 produced a robust response (Fig. 3E).

Agonist-internalised GLP-1Rs continue to generate cAMP signals from the endosomal compartment [45], with this process being ligand specific [46]. To monitor the distribution of GLP-1Rs in their active state between plasma membrane and endosomes with exendin-4, P5 and exendin-phe1, we co-expressed mini-G_s tagged with nanoluciferase with Venus-tagged markers of the plasma membrane (KRAS) or early endosome (Rab5) [26]. In this bystander configuration, the location of GLP-1R in its active conformation is inferred when mini-G_s is recruited to the vicinity of the relevant compartment marker leading to an increase in BRET signal. In stable HEK293-SNAP-GLP-1R cells, 100 nM exendin-4

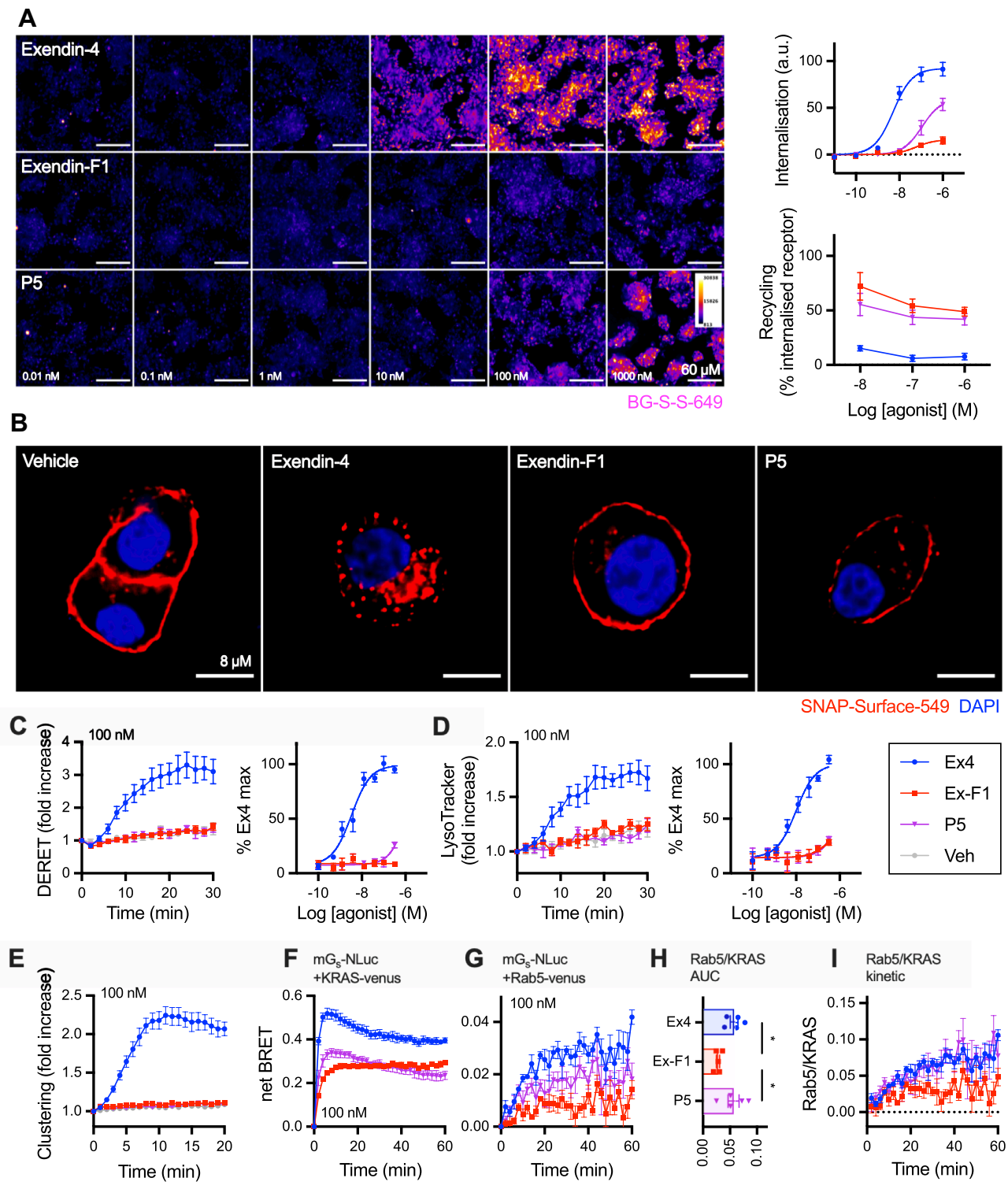

Fig. 3. Trafficking responses of biased GLP-1R agonists. (**A**) GLP-1R internalisation (30 min) and recycling (60 min) with each GLP-1R agonist in HEK293-SNAP-GLP-1R cells. Representative cropped images are shown for the internalisation step, with quantification from $n = 5$ experiments. Scale bar = 60 µm. (**B**) Representative high-resolution images showing GLP-1R internalisation in HEK293-SNAP-GLP-1R cells with 100 nM ligand, 30 min. Scale bar = 8 µm. (**C**) GLP-1R internalisation in HEK293-SNAP-GLP-1R cells measured by DERET, with kinetic response for 100 nM agonist shown and quantification from 30-min AUC also indicated, $n = 5$. (**D**) As for (C) but for GLP-1R trafficking to lysosomal compartment. (**E**) GLP-1R clustering in HEK293-SNAP-GLP-1R cells stimulated with 100 nM agonist, $n = 5$. (**F**) Recruitment of mini-G_s-Nluc to plasma membrane (KRAS-Venus marker) in HEK293-SNAP-GLP-1R cells stimulated with 100 nM agonist, $n = 5$. (**G**) As for (F) but recruitment to early endosomes (Rab5-Venus marker). (**H**) AUC ratio indicating balance of Rab5 to KRAS mini-G_s-Nluc BRET signals from (F) and (G), with statistical comparison by one-way randomised block ANOVA with Tukey's test. (**I**) Ratio of BRET signals from (F) and (G) expressed at each time-point. * $p < 0.05$ by indicated statistical test. Data are represented as mean ± SEM, with individual replicates shown where possible.

induced robust and rapid translocation of mini-G_s to the plasma membrane, followed by a gradual decline; a similar pattern, but with a lower peak, was seen with P5 (Fig. 3F). For exendin-F1, the peak response was further reduced, but did not fall below the peak level for the full 30-minute stimulation period. Mini-G_s recruitment to Rab5-positive early endosomes was of slower onset than at the plasma membrane, and response magnitude showed a rank order matching that of GLP-1R endocytosis (exendin-4 > P5 > exendin-F1; Fig. 3G). Expressing ligand-specific Rab5 and KRAS signals ratiometrically from their AUC (Fig. 3H), or over time (Fig. 3I), suggested P5 engenders a similar balance between endosomal and plasma membrane activity to exendin-4, but exendin-F1 delivers a predominantly plasma membrane delimited response. We did not attempt to perform full concentration responses with these assays due to the low dynamic range of the Rab5 BRET assay.

Therefore, both P5 and exendin-F1 show reduced GLP-1R endocytosis and accelerated recycling, with this effect being most dramatic for exendin-F1. The differences in GLP-1R internalisation between P5 and exendin-F1 are mirrored by their respective tendencies to elicit GLP-1R activity at early endosomes.

3.3. Beta cell and in vivo effects of exendin-F1 versus P5

GLP-1R-specific signalling was confirmed for each peptide by comparing acute cAMP responses in the pancreatic beta cell line INS-1 832/3 [21] and a CRISPR/Cas9-derived subclone thereof lacking endogenous GLP-1R or GIPR expression [22] (Fig. 4A, Table 2). Interestingly, efficacy with P5 was slightly higher than with the other two ligands in GLP-1R-expressing cells.

Previous work has demonstrated how prolonged stimulation with GLP-1R agonists with different trafficking phenotypes leads to variable levels of receptor downregulation, which can influence their insulinotropic potential [9,10]. In SNAP-GLP-1R stably expressed in INS-1 832/3 cells lacking endogenous GLP-1R, referred to as INS-1-SNAP-GLP-1R

Table 2
Parameter estimates for responses in beta cell models. Mean ± SEM for potency and efficacy estimates from Fig. 4. E_{max} values are reported as in the figure, i.e. as a % of forskolin response for INS-1 cAMP results, % remaining surface receptor for GLP-1R downregulation assay, and as fold change response *versus* 11 mM glucose for the insulin secretion assay. Statistical comparisons are by one-way randomised block ANOVA with Tukey's test. * $p < 0.05$ *versus* exendin-4; # $p < 0.05$ exendin-F1 *versus* P5. n.c. = not calculable.

	Exendin-4		Exendin-F1		P5	
Assay and cell model	pEC_{50} (M)	E_{max}	pEC_{50} (M)	E_{max}	pEC_{50} (M)	E_{max}
cAMP (INS-1 832/3, wild-type)	9.6 ± 0.1	76 ± 11	8.6 ± 0.2 *	74 ± 12	8.1 ± 0.2 *,#	91 ± 13 *,#
cAMP (INS-1 832/3, GLP-1R KO)	n.c.	n.c.	n.c.	n.c.	n.c.	n.c.
cAMP (INS-1 832/3, GIPR KO)	9.8 ± 0.1	76 ± 13	8.8 ± 0.2 *	80 ± 14	8.3 ± 0.2 *,#	93 ± 15 *,#
GLP-1R downregulation (INS-1-SNAP-GLP-1R)	9.2 ± 0.2	6 ± 2	7.7 ± 0.2 *	39 ± 5 *	6.6 ± 0.2 *,#	6 ± 3 #
Insulin secretion (INS-1 832/3)	10.3 ± 0.1	2.7 ± 0.3	9.4 ± 0.1 *	4.3 ± 0.3 *	9.1 ± 0.3 *	2.5 ± 0.4 #

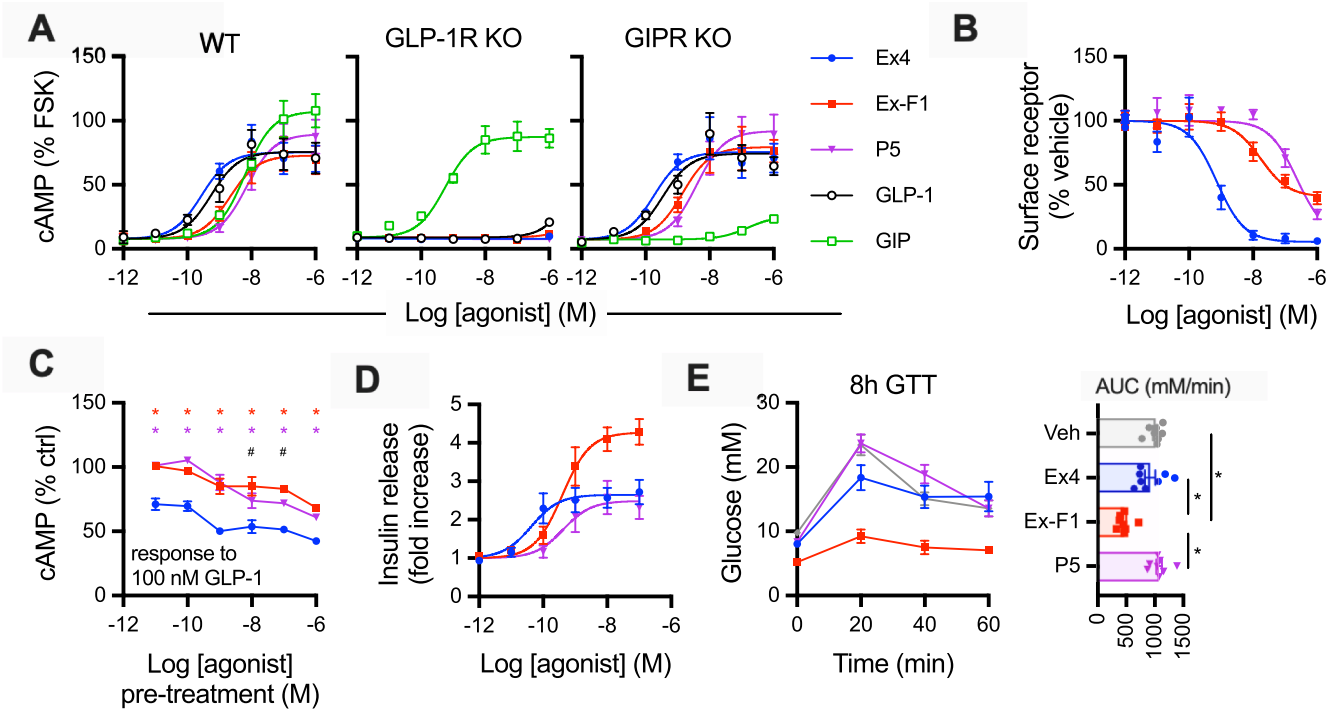

Fig. 4. Responses in beta cells and anti-hyperglycaemic efficacy. (**A**) Acute cAMP signalling in INS-1 832/3 cells with and without endogenous GLP-1R or GIPR, as indicated, for 10-min stimulation with 500 μM IBMX, expressed relative to forskolin (FSK; 10 μM) response, 3-parameter fits shown, $n = 4$. (**B**) Residual surface SNAP-GLP-1R after overnight treatment of INS-1 832/3 cells with indicated agonist concentrations, 3-parameter fits shown, $n = 5$. (**C**) Homologous desensitisation assay in INS-1 832/3 cells treated overnight with indicated agonist concentration, followed by a 1-hour recovery period and stimulation with 100 nM GLP-1 plus 500 μM IBMX, $n = 4$. Responses are expressed relative to vehicle pre-treated cells, with two-way randomised block ANOVA with Sidak's test performed. (**D**) Cumulative insulin secretion in INS-1 832/3 cells treated with indicated agonist overnight at 11 mM glucose, expressed as a fold change relative to response to zero agonist condition, $n = 5$. (**E**) Intraperitoneal glucose tolerance test (2 g/kg glucose) performed in lean male C57Bl/6 mice, 8 h after administration of 2.4 nmol/kg agonist, $n = 8$ per group, with AUC comparisons by one-way ANOVA with Tukey's test. * $p < 0.05$ by indicated statistical test; for (C), red asterisk indicates exendin-F1 *versus* exendin-4, purple asterisk indicates P5 *versus* exendin-4, # indicates exendin-F1 *versus* P5. Data are represented as mean ± SEM, with individual replicates shown where possible. (For interpretation of the references to colour in this figure legend, the reader is referred to the web version of this article.)

cells [47], both exendin-F1 and P5 showed markedly increased preservation of surface GLP-1R levels compared to exendin-4 (Fig. 4B, Table 2). Exendin-F1 led to loss of surface GLP-1R at lower concentrations than P5, as expected from its higher affinity, but the maximum loss of surface receptor effect was less marked.

To determine the functional impact of differential GLP-1R downregulation, we measured cAMP responses to a fixed concentration of GLP-1 after a prior 16-hour pre-treatment phase with each exendin analogue. Both biased ligands produced substantially less homologous desensitisation than exendin-4 (Fig. 4C). Whilst concentration responses could not be accurately quantified by logistic curve fitting of data from assay repeats, P5 showed greater desensitisation than exendin-F1 at pre-treatment concentrations upwards of 10 nM.

We also measured cumulative insulin secretion with each ligand after an overnight stimulation as a therapeutically relevant readout of sustained pharmacological agonism in beta cells. Here, there was a stark difference in insulinotropic efficacy, with exendin-F1 treatment yielding approximately twice as much insulin secretion as exendin-4 and P5 (Fig. 4D, Table 2). Moreover, assessment of anti-hyperglycaemic efficacy in mice by intraperitoneal glucose tolerance testing, performed 8 h after agonist administration to allow desensitisation-related effects to emerge as previously performed [9,10], showed a pattern compatible with apparent greater sustained action with exendin-F1 (Fig. 4E). Note that both P5 and exendin-F1 have been demonstrated to show identical pharmacokinetics to exendin-4 [8,9].

4. Discussion

In this study we have compared two exendin-4 analogues, P5 and exendin-F1, that were the first two synthetic, orthosteric GLP-1RAs reported to show biased agonism favouring G protein-dependent signalling over β-arrestin recruitment and tested *in vivo* for their metabolic effects. Biased GLP-1R agonism has emerged as a promising therapeutic strategy for T2D on the basis of preclinical evaluations [8,9,11] and the recent recognition that some of the beneficial effects of the dual GLP-1R/GIPR agonist tirzepatide may be due to biased agonism at the GLP-1R [14]. Whilst in our study we confirmed the exendin-F1 and P5 do indeed show selective reduction in β-arrestin recruitment, their patterns of engagement with intracellular effectors, trafficking profiles, subcellular signalling localisation and insulinotropic efficacy were in fact rather different.

It is notable that both exendin-F1 and P5, considered G protein-biased from previous reports [8,9], are in fact low efficacy agonists for mini-G_s engagement compared to the full agonist exendin-4. We verified bias in favour of cAMP production over β-arrestin-2 recruitment in the PathHunter system, but interestingly, the same operational analysis did not indicate bias between mini-G_s and β-arrestin-2 recruitment for P5 (while for exendin-F1 the β-arrestin-2 response was undetectable, precluding formal analysis). There is increasing recognition that bias comparisons between readouts encompassing significant signal amplification (e.g. cAMP) and those without amplification (e.g. β-arrestin recruitment) are susceptible to system non-linearity that may confound current models [48,49]. However, if seen from the pragmatic point of view that efficacy is a key driver of the manifestations of biased agonism [48], considering P5 and exendin-F1 as G protein-biased appear appropriate, as in both cases β-arrestin-2 recruitment is even more markedly reduced than mini-G_s recruitment.

Our whole cell binding assays indicated lower affinity for P5 than for exendin-F1. Indeed, P5 was previously identified as a low affinity agonist, with a reported ~ 100-fold lower affinity than GLP-1 in competition with iodinated exendin(9–39) [40]. Our P5 pK_i measurements were dependent on the choice of competing fluorescent probe, with apparently lower affinity measured when the antagonist LUXendin645 was used rather than the equivalent agonist exendin-4-Cy5. In a previous report, the absence of G proteins, or expression of a dominant negative $G\alpha_s$, led to smaller differences between P5 and exendin-4 affinity in insect cells [40]. Thus, probe-dependency of measured pK_i with P5 could represent a higher affinity GLP-1R active-state complex triggered by exendin-4-Cy5-induced coupling to $G\alpha_s$ that is not seen with LUXendin645 [50]. Additionally, whilst our whole cell binding assays were performed at low temperature and with metabolic inhibitors to avoid the effects of ATP-dependent GLP-1R redistribution and endocytosis on binding phenomena, we cannot absolutely exclude these as ligand-specific confounders. Affinity measurements in cell-free reconstituted systems could be performed to address this issue.

Contrasting with its higher affinity, maximum responses for multiple readouts were further reduced for exendin-F1 than for P5. Thus, recruitment of mini-G_s, GRK2 and β-arrestin-2 to the receptor, and activation of $G\alpha_s$ as measured by Nb37 recruitment to SNAP-GLP-1R-Nluc, were measurably lower with high doses of exendin-F1 *versus* P5, as was GLP-1R endocytosis. The counterbalancing of effects on affinity *versus* efficacy appears to result in similar acute cAMP potency estimates for both ligands (albeit slightly reduced with P5, depending on the cell system), with P5 relying on greater coupling to intracellular effectors in the face of lower affinity. This distinction may be important as efficacy-*versus* affinity-driven signalling can manifest differently in tissues with greater or lesser sensitivity to GLP-1R stimulation, due to factors such as expression levels of GLP-1R, signalling intermediates and downstream effectors [51]. Specifically, in the presence of adequate GLP-1R expression, the low acute efficacy for both G protein and β-arrestin engagement of exendin-F1 is still sufficient to fully activate cAMP/PKA signalling either due to either signal amplification or differences in capacity to induce activation of recruited G proteins, whilst at the same time avoiding β-arrestin-mediated desensitisation and downregulation phenomena that otherwise limit response duration. In contrast, the same ligand might fail to induce high amplitude responses in tissues with lower GLP-1R expression (see Fig. 5). This tissue selectivity could potentially influence the risk of side effects when used therapeutically.

After endocytosis, a number of GPCRs are known to continue to signal from the endosomal compartment [52]. Pharmacological and genetic inhibition of GLP-1R endocytosis attenuates cAMP production [53,54], and $G\alpha_s$ was found to colocalise with GLP-1R in early endosomes [45]. In our study, we have monitored ligand-specific patterns of redistribution of GLP-1R in its $G\alpha_s$-preferring active conformation from the plasma membrane to early endosomes. Here, P5 led to more active GLP-1Rs at Rab5-positive early endosomes than exendin-F1, in line with the greater total GLP-1R internalisation recorded with this ligand. This could be important given that "location bias" can modulate agonist effects, as the same intracellular signalling events originating at the endosome *versus* plasma membrane may result in distinct downstream actions [55]. Endosomal signalling is often referred to as being responsible for sustained responses [56]. However, our results call into question the relative importance of this phenomenon in controlling the duration of action of GLP-1RAs in the therapeutic setting, as exendin-F1 showed the least tendency to promote GLP-1R activation at the endosomal compartment but the greatest maximal insulin secretion after prolonged incubation with beta cells, and a greater glucose-lowering effect than P5 in a delayed glucose tolerance test in mice. This is presumably attributable to a sufficiently enhanced avoidance of receptor desensitisation and downregulation, both of which ultimately limit the global capacity for signalling for the GLP-1R, to the point that any potential advantages of endosomal signalling no longer dominate. Ultimately, the balance between the positive and negative contributions of all the above-mentioned factors is likely to determine the overall capacity of each pharmacological agonist for sustained action.

Despite its reduced importance in a pharmacological setting, endosomal signalling is likely to play a more prominent role in mediating physiological GLP-1R effects, as the lower plasma concentrations and short circulatory half-life of GLP-1 and other proglucagon-derived peptides means that the fraction of downregulated GLP-1R is likely to be minimal. Moreover, it should be emphasised that our mini-G_s bystander BRET assay does not measure endosomal signalling *per se,* but

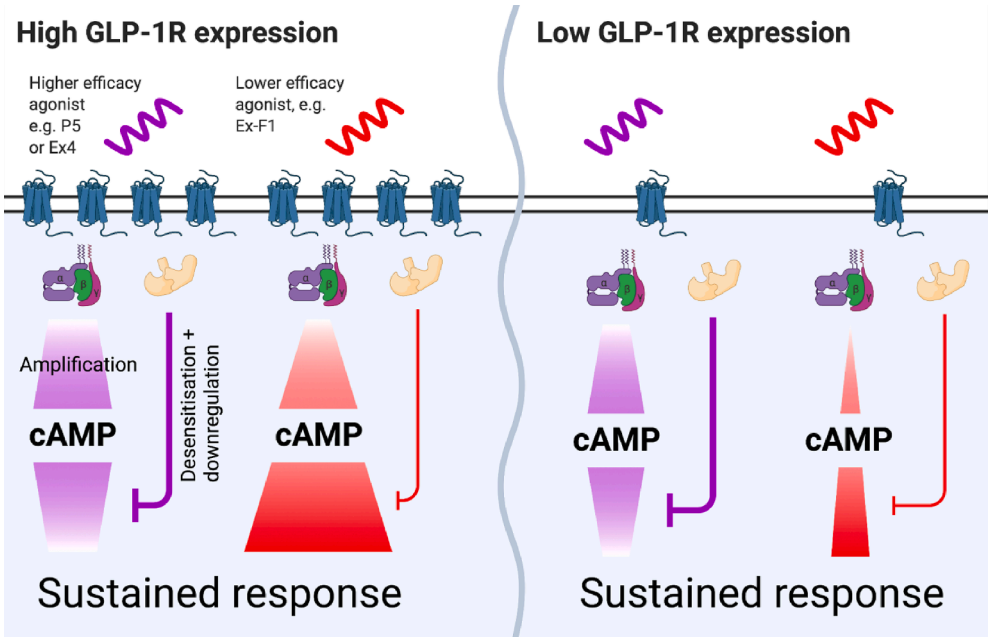

Fig. 5. Possible effects of tissue-specific GLP-1R expression levels on downstream responses. With high levels of GLP-1R surface expression, the modest degree of $G\alpha_s$ recruitment with the low efficacy agonist exendin-F1 is amplified sufficiently to generate a full cAMP response and, in the absence of substantial desensitisation or downregulation, a high efficacy biological response is achieved after prolonged stimulation. This allows the agonist to "outperform" the higher acute efficacy agonist P5, e.g. for insulin secretion. Exendin-4, as a high efficacy agonist, behaves more like P5 in this assay. When GLP-1R expression levels are low, the absolute $G\alpha_s$ recruitment response with exendin-F1 is too small to achieve a full downstream response, even with amplification. Physiologically relevant outputs from low-expression tissues may therefore show a smaller difference between agonists or changes to rank order. Several other factors beyond receptor density are almost certain to influence these processes, including receptor organisation within the plasma membrane or changes in plasma membrane lipid composition, expression of relevant effectors, and sensitivity of downstream pathways. Image created using Biorender.

the presence of activated GLP-1R at particular locations. Targeted biosensors to monitor cAMP generation [46] or PKA activation [57] are available, and Nb37 redistribution can be observed by microscopy [27], although these tend to be lower throughput methods.

At the outset of the present study, we anticipated that P5 would in fact be highly insulinotropic when assessed using the same methodology [9] used to reveal the impact of GLP-1R desensitisation and time-dependent advantages of exendin-F1, but this proved not to be the case. It appears that P5 achieves a less favourable balance between "beneficial" signalling and "non-beneficial" desensitisation which ultimately limits the amplitude of the sustained insulin release response, which was in fact similar to that of exendin-4. The potent effects of P5 on blood glucose lowering reported by Zhang *et al* [8] were observed in the "hyper-acute" setting, i.e. with a different approach to the delayed IPGTT used in our study, as well as being corroborated by improvements in HbA1c after chronic administration. Our results do not shed any light on how P5 obtains its pronounced anti-hyperglycaemic effects, which remain hard to explain as P5 was less insulinotropic than exendin-4 and had no differential effect on insulin sensitivity. An insulin-independent mechanism remains a possibility but was not explored in the study of Zhang *et al* [8]. Chronic treatment with P5 led to various metabolic changes that exceed those of the same dose of exendin-4, including increased adipose tissue hyperplasia and reduced inflammation, along with increased circulating GIP and reduced circulating resistin [8]. These may be relevant in the chronic setting but unlikely to contribute to the hyperacute effects of P5 on glucose levels.

In summary, whilst P5 and exendin-F1 superficially resemble each other at the pharmacological level, our study highlights that emphasising lower acute efficacy for transducer coupling, but higher affinity or potency, may be a more viable strategy to achieve therapeutically optimised GLP-1R biased agonism.

CRediT authorship contribution statement

Amaara Marzook: Investigation, Formal analysis, Writin, g - review & editing, Visualization. **Shiqian Chen:** Investigation, Formal analysis, Writing - review & editing. **Phil Pickford:** Investigation, Formal analysis, Writing - review & editing. **Maria Lucey:** Investigation, Formal analysis, Writing - review & editing. **Yifan Wang:** Investigation, Writing - review & editing. **Ivan R. Corrêa Jr:** Resources, Writing - review & editing. **Johannes Broichhagen:** Resources, Writing - review & editing. **David J. Hodson:** Resources, Writing - review & editing. **Victoria Salem:** Supervision, Writing - review & editing. **Guy A. Rutter:** Funding acquisition, Writing - review & editing. **Tricia M. Tan:** Supervision, Writing - review & editing. **Stephen R. Bloom:** Funding acquisition, Writing - review & editing. **Alejandra Tomas:** Conceptualization, Funding acquisition, Writing - review & editing. **Ben Jones:** Conceptualization, Funding acquisition, Investigation, Formal analysis, Writing - original draft, Visualization, Project administration.

Declaration of Competing Interest

G.A.R., A.T. and B.J. have received grant funding from Sun Pharmaceuticals.

Acknowledgements

The Section of Endocrinology and Investigative Medicine is funded by grants from the MRC, BBSRC, NIHR, and is supported by the NIHR Biomedical Research Centre Funding Scheme. The views expressed are those of the authors and not necessarily those of the funders. This project was supported by an MRC project grant (MR/R010676/1) to A.T., B.J., S.R.B., and G.A.R. The European Federation for the Study of Diabetes has supported B.J. and A.T. in this work. A.T. also acknowledges funding from Diabetes UK. B.J. acknowledges support from the Academy of Medical Sciences, Society for Endocrinology, The British Society for Neuroendocrinology, the European Federation for the Study of Diabetes, and an EPSRC capital award. D.J.H. was supported by MRC (MR/N00275X/1 and MR/S025618/1) and Diabetes UK (17/0005681) Project Grants. This project has received funding from the European Research Council (ERC) under the European Union's Horizon 2020 research and innovation programme (Starting Grant 715884 to D.J.H.). G.A.R. was supported by Wellcome Trust Investigator (212625/Z/18/Z) Awards, MRC Programme (MR/R022259/1) and Experimental Challenge Grant (DIVA, MR/L02036X/1), and Diabetes UK (BDA/11/0004210, BDA/15/0005275, BDA 16/0005485) grants. This work has

received support from the EU/EFPIA/Innovative Medicines Initiative 2 Joint Undertaking (RHAPSODY grant No 115881) to G.A.R. V.S. was supported by a Diabetes UK Harry Keen Fellowship.

References

[1] N.H. Cho, J.E. Shaw, S. Karuranga, Y. Huang, J.D. da Rocha Fernandes, A.W. Ohlrogge, et al., IDF Diabetes Atlas: Global estimates of diabetes prevalence for 2017 and projections for 2045, Diabetes Res. Clin. Pract. (2018). doi:10.1016/j.diabres.2018.02.023.

[2] M. Stumvoll, B.J. Goldstein, T.W. van Haeften, Type 2 diabetes: principles of pathogenesis and therapy, Lancet 365 (9467) (2005) 1333–1346, https://doi.org/10.1016/S0140-6736(05)61032-X.

[3] D.J. Drucker, Mechanisms of action and therapeutic application of glucagon-like peptide-1, Cell Metab. 27 (4) (2018) 740–756, https://doi.org/10.1016/j.cmet.2018.03.001.

[4] T.D. Müller, B. Finan, S.R. Bloom, D. D'Alessio, D.J. Drucker, P.R. Flatt, A. Fritsche, F. Gribble, H.J. Grill, J.F. Habener, J.J. Holst, W. Langhans, J.J. Meier, M.A. Nauck, D. Perez-Tilve, A. Pocai, F. Reimann, D.A. Sandoval, T.W. Schwartz, R.J. Seeley, K. Stemmer, M. Tang-Christensen, S.C. Woods, R.D. DiMarchi, M.H. Tschöp, Glucagon-like peptide 1 (GLP-1), Mol. Metab. 30 (2019) 72–130, https://doi.org/10.1016/j.molmet.2019.09.010.

[5] J. Eng, W.A. Kleinman, L. Singh, G. Singh, J.P. Raufman, Isolation and characterization of exendin-4, an exendin-3 analogue, from Heloderma suspectum venom. Further evidence for an exendin receptor on dispersed acini from guinea pig pancreas, J. Biol. Chem. 267 (11) (1992) 7402–7405.

[6] M.A. Bethel, R.A. Patel, P. Merrill, Y. Lokhnygina, J.B. Buse, R.J. Mentz, N. J. Pagidipati, J.C. Chan, S.M. Gustavson, N. Iqbal, A.P. Maggioni, P. Öhman, N. R. Poulter, A. Ramachandran, B. Zinman, A.F. Hernandez, R.R. Holman, Cardiovascular outcomes with glucagon-like peptide-1 receptor agonists in patients with type 2 diabetes: a meta-analysis, Lancet Diabetes Endocrinol. 6 (2) (2018) 105–113, https://doi.org/10.1016/S2213-8587(17)30412-6.

[7] S.L. Zheng, A.J. Roddick, R. Aghar-Jaffar, M.J. Shun-Shin, D. Francis, N. Oliver, K. Meeran, Association between use of sodium-glucose cotransporter 2 inhibitors, glucagon-like peptide 1 agonists, and dipeptidyl peptidase 4 inhibitors with all-cause mortality in patients with type 2 diabetes: a systematic review and meta-analysis, JAMA 319 (15) (2018) 1580, https://doi.org/10.1001/jama.2018.3024.

[8] H. Zhang, E. Sturchler, J. Zhu, A. Nieto, P.A. Cistrone, J. Xie, LinLing He, K. Yea, T. Jones, R. Turn, P.S. Di Stefano, P.R. Griffin, P.E. Dawson, P.H. McDonald, R. A. Lerner, Autocrine selection of a GLP-1R G-protein biased agonist with potent antidiabetic effects, Nat. Commun. 6 (1) (2015), https://doi.org/10.1038/ncomms9918.

[9] B. Jones, T. Buenaventura, N. Kanda, P. Chabosseau, B.M. Owen, R. Scott, R. Goldin, N. Angkathunyakul, I.R. Corrêa Jr, D. Bosco, P.R. Johnson, L. Piemonti, P. Marchetti, A.M.J. Shapiro, B.J. Cochran, A.C. Hanyaloglu, A. Inoue, T. Tan, G. A. Rutter, A. Tomas, S.R. Bloom, Targeting GLP-1 receptor trafficking to improve agonist efficacy, Nat. Commun. 9 (1) (2018), https://doi.org/10.1038/s41467-018-03941-2.

[10] J. Fremaux, C. Venin, L. Mauran, R. Zimmer, F. Koensgen, D. Rognan, S. Bitsi, M. A. Lucey, B. Jones, A. Tomas, G. Guichard, S.R. Goudreau, Ureidopeptide GLP-1 analogues with prolonged activity in vivo via signal bias and altered receptor trafficking, Chem. Sci. 10 (42) (2019) 9872–9879, https://doi.org/10.1039/C9SC02079A.

[11] M. Lucey, P. Pickford, S. Bitsi, J. Minnion, J. Ungewiss, K. Schoeneberg, G. A. Rutter, S.R. Bloom, A. Tomas, B. Jones, Disconnect between signalling potency and in vivo efficacy of pharmacokinetically optimised biased glucagon-like peptide-1 receptor agonists, Mol. Metab. 37 (2020) 100991, https://doi.org/10.1016/j.molmet.2020.100991.

[12] M. Wang, P. Yao, M. Gao, J. Jin, Y. Yu, Novel fatty chain-modified GLP-1R G-protein biased agonist exerts prolonged anti-diabetic effects through targeting receptor binding sites, RSC Adv. 10 (14) (2020) 8044–8053, https://doi.org/10.1039/C9RA10593J.

[13] E. Yuliantie, S. Darbalaei, A. Dai, P. Zhao, D. Yang, P.M. Sexton, et al., Pharmacological characterization of mono-, dual- and tri- peptidic agonists at GIP and GLP-1 receptors, Biochem. Pharmacol. 2020 114001. doi:10.1016/j.bcp.2020.114001.

[14] F.S. Willard, J.D. Douros, M.B. Gabe, A.D. Showalter, D.B. Wainscott, T.M. Suter, et al., Tirzepatide is an imbalanced and biased dual GIP and GLP-1 receptor agonist, JCI Insight. 5 220 1202. doi:10.1172/jci.insight.140532.

[15] A. Novikoff, S.L. O'Brien, M. Bernecker, G. Grandl, M. Kleinert, P.J. Knerr, et al., Spatiotemporal GLP-1 and GIPR receptor signaling and trafficking/recycling dynamics induced by selected receptor mono- and dual-agonists, Mol. Metab. (2021), 101181, https://doi.org/10.1016/j.molmet.2021.101181.

[16] J.P. Frias, M.A. Nauck, J. Van, M.E. Kutner, X. Cui, C. Benson, S. Urva, R. E. Gimeno, Z. Milicevic, D. Robins, A. Haupt, Efficacy and safety of LY3298176, a novel dual GIP and GLP-1 receptor agonist, in patients with type 2 diabetes: a randomised, placebo-controlled and active comparator-controlled phase 2 trial, Lancet 392 (10160) (2018) 2180–2193, https://doi.org/10.1016/S0140-6736(18)32260-8.

[17] C.M. Costa-Neto, L.T. Parreiras-e-Silva, M. Bouvier, A pluridimensional view of biased agonism, Mol. Pharmacol. 90 (5) (2016) 587–595, https://doi.org/10.1124/mol.116.105940.

[18] Z. Fang, S. Chen, Y. Manchanda, S. Bitsi, P. Pickford, A. David, M.M. Shchepinova, I.R. Corrêa Jr, D.J. Hodson, J. Broichhagen, E.W. Tate, F. Reimann, V. Salem, G. A. Rutter, T. Tan, S.R. Bloom, A. Tomas, B. Jones, Ligand-specific factors influencing GLP-1 receptor post-endocytic trafficking and degradation in pancreatic beta cells, Int. J. Mol. Sci. 21 (21) (2020) 8404, https://doi.org/10.3390/ijms21218404.

[19] J. Ast, A. Arvaniti, N.H.F. Fine, D. Nasteska, F.B. Ashford, Z. Stamataki, Z. Koszegi, A. Bacon, B.J. Jones, M.A. Lucey, S. Sasaki, D.I. Brierley, B. Hastoy, A. Tomas, G. D'Agostino, F. Reimann, F.C. Lynn, C.A. Reissaus, A.K. Linnemann, E. D'Este, D. Calebiro, S. Trapp, K. Johnsson, T. Podewin, J. Broichhagen, D.J. Hodson, Super-resolution microscopy compatible fluorescent probes reveal endogenous glucagon-like peptide-1 receptor distribution and dynamics, Nat. Commun. 11 (1) (2020), https://doi.org/10.1038/s41467-020-14309-w.

[20] T. Buenaventura, S. Bitsi, W.E. Laughlin, T. Burgoyne, Z. Lyu, A.I. Oqua, H. Norman, E.R. McGlone, A.S. Klymchenko, I.R. Corrêa, A. Walker, A. Inoue, A. Hanyaloglu, J. Grimes, Z. Koszegi, D. Calebiro, G.A. Rutter, S.R. Bloom, B. Jones, A. Tomas, P. Titchenell, Agonist-induced membrane nanodomain clustering drives GLP-1 receptor responses in pancreatic beta cells, PLoS Biol. 17 (8) (2019) e3000097, https://doi.org/10.1371/journal.pbio.3000097.

[21] H.E. Hohmeier, H. Mulder, G. Chen, R. Henkel-Rieger, M. Prentki, C.B. Newgard, Isolation of INS-1-derived cell lines with robust ATP-sensitive K+ channel-dependent and -independent glucose-stimulated insulin secretion, Diabetes 49 (3) (2000) 424–430.

[22] J. Naylor, A.T. Suckow, A. Seth, D.J. Baker, I. Sermadiras, P. Ravn, et al., Use of CRISPR/Cas9-engineered INS-1 pancreatic β cells to define the pharmacology of dual GIPR/GLP-1R agonists, Biochem. J. 473 2016 2881–2891. doi:10.1042/BCJ20160476.

[23] C. Widmann, W. Dolci, B. Thorens, Agonist-induced internalization and recycling of the glucagon-like peptide-1 receptor in transfected fibroblasts and in insulinomas, Biochem. J. 310 (Pt 1) (1995) 203–214.

[24] D.I. Danylchuk, S. Moon, K.e. Xu, A.S. Klymchenko, Switchable solvatochromic probes for live-cell super-resolution imaging of plasma membrane organization, Angew. Chem. Int. Ed. Engl. 58 (42) (2019) 14920–14924, https://doi.org/10.1002/anie.v58.4210.1002/anie.201907690.

[25] Z. Fang, S. Chen, P. Pickford, J. Broichhagen, D.J. Hodson, I.R. Corrêa, S. Kumar, F. Görlitz, C. Dunsby, P.M.W. French, G.A. Rutter, T. Tan, S.R. Bloom, A. Tomas, B. Jones, The influence of peptide context on signaling and trafficking of glucagon-like peptide-1 receptor biased agonists, ACS Pharmacol. Transl. Sci. 3 (2) (2020) 345–360, https://doi.org/10.1021/acsptsci.0c0002210.1021/acsptsci.0c00022.s001.

[26] Q. Wan, N. Okashah, A. Inoue, R. Nehmé, B. Carpenter, C.G. Tate, N.A. Lambert, Mini G protein probes for active G protein-coupled receptors (GPCRs) in live cells, J. Biol. Chem. 293 (19) (2018) 7466–7473, https://doi.org/10.1074/jbc.RA118.001975.

[27] R. Irannejad, J.C. Tomshine, J.R. Tomshine, M. Chevalier, J.P. Mahoney, J. Steyaert, S.G.F. Rasmussen, R.K. Sunahara, H. El-Samad, B.o. Huang, M. von Zastrow, Conformational biosensors reveal GPCR signalling from endosomes, Nature 495 (7442) (2013) 534–538, https://doi.org/10.1038/nature12000.

[28] A. Oishi, J. Dam, R. Jockers, β-Arrestin-2 BRET Biosensors Detect Different β-Arrestin-2 Conformations in Interaction with GPCRs, ACS Sens. (2019) acssensors.9b01414. doi:10.1021/acssensors.9b01414.

[29] D. Sage, L. Donati, F. Soulez, D. Fortun, G. Schmit, A. Seitz, R. Guiet, C. Vonesch, M. Unser, DeconvolutionLab2: An open-source software for deconvolution microscopy, Methods 115 (2017) 28–41, https://doi.org/10.1016/j.ymeth.2016.12.015.

[30] A. Edelstein, N. Amodaj, K. Hoover, R. Vale, N. Stuurman, Computer control of microscopes using μManager, Curr Protoc Mol Biol. Chapter 14 (2010) Unit14.20. doi:10.1002/0471142727.mb1420s92.

[31] N. Jaccard, L.D. Griffin, A. Keser, R.J. Macown, A. Super, F.S. Veraitch, N. Szita, Automated method for the rapid and precise estimation of adherent cell culture characteristics from phase contrast microscopy images, Biotechnol. Bioeng. 111 (3) (2014) 504–517, https://doi.org/10.1002/bit.v111.310.1002/bit.25115.

[32] T. Peng, K. Thorn, T. Schroeder, L. Wang, F.J. Theis, C. Marr, et al., A BaSiC tool for background and shading correction of optical microscopy images, Nat. Commun. 8 (2017) 14836–14837, https://doi.org/10.1038/ncomms14836.

[33] T. Kenakin, C. Watson, V. Muniz-Medina, A. Christopoulos, S. Novick, A simple method for quantifying functional selectivity and agonist bias, ACS Chem. Neurosci. 3 (3) (2012) 193–203, https://doi.org/10.1021/cn200111m.

[34] E.T. van der Westhuizen, B. Breton, A. Christopoulos, M. Bouvier, Quantification of ligand bias for clinically relevant β2-adrenergic receptor ligands: implications for drug taxonomy, Mol. Pharmacol. 85 (3) (2014) 492–509, https://doi.org/10.1124/mol.113.088880.

[35] P. Pickford, M. Lucey, Z. Fang, S. Bitsi, J.B. Serna, J. Broichhagen, D.J. Hodson, J. Minnion, G.A. Rutter, S.R. Bloom, A. Tomas, B. Jones, Signalling, trafficking and glucoregulatory properties of glucagon-like peptide-1 receptor agonists exendin-4 and lixisenatide, Br. J. Pharmacol. 177 (17) (2020) 3905–3923, https://doi.org/10.1111/bph.v177.1710.1111/bph.15134.

[36] M. Lucey, T. Ashik, A. Marzook, Y. Wang, J. Goulding, A. Oishi, et al., Acylation of the incretin peptide exendin-4 directly impacts GLP-1 receptor signalling and trafficking, bioRxiv. (2021) 2021.04.01.438030. doi:10.1101/2021.04.01.438030.

[37] I. Ziomkiewicz, A. Loman, R. Klement, C. Fritsch, A.S. Klymchenko, G. Bunt, et al., Dynamic conformational transitions of the EGF receptor in living mammalian cells determined by FRET and fluorescence lifetime imaging microscopy, Cytometry A. 83 (2013) 794–805, https://doi.org/10.1002/cyto.a.22311.

[38] F. Wu, L. Yang, K. Hang, M. Laursen, L. Wu, G.W. Han, Q. Ren, N.K. Roed, G. Lin, M.A. Hanson, H. Jiang, M.-W. Wang, S. Reedtz-Runge, G. Song, R.C. Stevens, Full-length human GLP-1 receptor structure without orthosteric ligands, Nat. Commun. 11 (1) (2020), https://doi.org/10.1038/s41467-020-14934-5.

[39] X. Zhang, M.J. Belousoff, P. Zhao, A.J. Kooistra, T.T. Truong, S.Y. Ang, C. R. Underwood, T. Egebjerg, P. Šenel, G.D. Stewart, Y.-L. Liang, A. Glukhova, H. Venugopal, A. Christopoulos, S.G.B. Furness, L.J. Miller, S. Reedtz-Runge, C. J. Langmead, D.E. Gloriam, R. Danev, P.M. Sexton, D. Wootten, Differential GLP-1R binding and activation by peptide and non-peptide agonists, Mol. Cell. 80 (3) (2020) 485–500.e7, https://doi.org/10.1016/j.molcel.2020.09.020.

[40] Y.-L. Liang, M. Khoshouei, A. Glukhova, S.G.B. Furness, P. Zhao, L. Clydesdale, C. Koole, T.T. Truong, D.M. Thal, S. Lei, M. Radjainia, R. Danev, W. Baumeister, M.-W. Wang, L.J. Miller, A. Christopoulos, P.M. Sexton, D. Wootten, Phase-plate cryo-EM structure of a biased agonist-bound human GLP-1 receptor-Gs complex, Nature 555 (7694) (2018) 121–125, https://doi.org/10.1038/nature25773.

[41] A.S. Dixon, M.K. Schwinn, M.P. Hall, K. Zimmerman, P. Otto, T.H. Lubben, B. L. Butler, B.F. Binkowski, T. Machleidt, T.A. Kirkland, M.G. Wood, C.T. Eggers, L. P. Encell, K.V. Wood, NanoLuc Complementation Reporter Optimized For Accurate Measurement Of Protein Interactions In Cells, ACS Chem. Biol. 11 (2) (2016) 400–408, https://doi.org/10.1021/acschembio.5b0075310.1021/acschembio.5b00753.s001.

[42] R. Jorgensen, V. Kubale, M. Vrecl, T.W. Schwartz, C.E. Elling, Oxyntomodulin differentially affects glucagon-like peptide-1 receptor beta-arrestin recruitment and signaling through Galpha(s), J. Pharmacol. Exp. Ther. 322 (2007) 148–154, https://doi.org/10.1124/jpet.107.120006.

[43] S. Al-Sabah, M. Al-Fulaij, G. Shaaban, H.A. Ahmed, R.J. Mann, D. Donnelly, M. Bünemann, C. Krasel, C. Holscher, The GIP receptor displays higher basal activity than the GLP-1 receptor but does not recruit GRK2 or arrestin3 effectively, PLoS One 9 (9) (2014) e106890, https://doi.org/10.1371/journal.pone.0106890.

[44] S.N. Roed, P. Wismann, C.R. Underwood, N. Kulahin, H. Iversen, K.A. Cappelen, L. Schäffer, J. Lehtonen, J. Hecksher-Soerensen, A. Secher, J.M. Mathiesen, H. Bräuner-Osborne, J.L. Whistler, S.M. Knudsen, M. Waldhoer, Real-time trafficking and signaling of the glucagon-like peptide-1 receptor, Mol. Cell Endocrinol. 382 (2) (2014) 938–949, https://doi.org/10.1016/j.mce:2013.11.010.

[45] S.B. Girada, R.S. Kuna, S. Bele, Z. Zhu, N.R. Chakravarthi, R.D. DiMarchi, P. Mitra, Gαs regulates Glucagon-Like Peptide 1 Receptor-mediated cyclic AMP generation at Rab5 endosomal compartment, Mol. Metab. 6 (10) (2017) 1173–1185, https://doi.org/10.1016/j.molmet.2017.08.002.

[46] M.M. Fletcher, M.L. Halls, P. Zhao, L. Clydesdale, A. Christopoulos, P.M. Sexton, D. Wootten, Glucagon-like peptide-1 receptor internalisation controls spatiotemporal signalling mediated by biased agonists, Biochem. Pharmacol. 156 (2018) 406–419, https://doi.org/10.1016/j.bcp.2018.09.003.

[47] T. Buenaventura, N. Kanda, P.C. Douzenis, B. Jones, S.R. Bloom, P. Chabosseau, I. R. Corrêa, D. Bosco, L. Piemonti, P. Marchetti, P.R. Johnson, A.M.J. Shapiro, G. A. Rutter, A. Tomas, A targeted RNAi screen identifies endocytic trafficking factors that control GLP-1 receptor signaling in pancreatic β-cells, Diabetes 67 (3) (2018) 385–399, https://doi.org/10.2337/db17-0639.

[48] H.O. Onaran, C. Ambrosio, Ö. Uğur, E. Madaras Koncz, M.C. Grò, V. Vezzi, S. Rajagopal, T. Costa, Systematic errors in detecting biased agonism: analysis of current methods and development of a new model-free approach, Sci. Rep. 7 (1) (2017), https://doi.org/10.1038/srep44247.

[49] A.E. Conibear, E. Kelly, A biased view of μ-opioid receptors? Mol. Pharmacol. 96 (5) (2019) 542–549, https://doi.org/10.1124/mol.119.115956.

[50] X.J. Yao, G. Velez Ruiz, M.R. Whorton, S.G.F. Rasmussen, B.T. DeVree, X. Deupi, R. K. Sunahara, B. Kobilka, The effect of ligand efficacy on the formation and stability of a GPCR-G protein complex, Proc. Natl. Acad. Sci. USA 106 (23) (2009) 9501–9506, https://doi.org/10.1073/pnas.0811437106.

[51] T. Kenakin, Is the quest for signaling bias worth the effort? Mol. Pharmacol. 93 (4) (2018) 266–269, https://doi.org/10.1124/mol.117.111187.

[52] A.R.B. Thomsen, D.D. Jensen, G.A. Hicks, N.W. Bunnett, Therapeutic targeting of endosomal G-protein-coupled receptors, Trends Pharmacol. Sci. 39 (10) (2018) 879–891, https://doi.org/10.1016/j.tips.2018.08.003.

[53] R.S. Kuna, S.B. Girada, S. Asalla, J. Vallentyne, S. Maddika, J.T. Patterson, D. L. Smiley, R.D. DiMarchi, P. Mitra, Glucagon-like peptide-1 receptor-mediated endosomal cAMP generation promotes glucose-stimulated insulin secretion in pancreatic β-cells, Am. J. Physiol. Endocrinol. Metab. 305 (2) (2013) E161–E170, https://doi.org/10.1152/ajpendo.00551.2012.

[54] S.N. Roed, A.C. Nøhr, P. Wismann, H. Iversen, H. Bräuner-Osborne, S.M. Knudsen, M. Waldhoer, Functional consequences of glucagon-like peptide-1 receptor cross-talk and trafficking, J. Biol. Chem. 290 (2) (2015) 1233–1243, https://doi.org/10.1074/jbc.M114.592436.

[55] R. Irannejad, V. Pessino, D. Mika, B.o. Huang, P.B. Wedegaertner, M. Conti, M. von Zastrow, Functional selectivity of GPCR-directed drug action through location bias, Nat. Chem. Biol. 13 (7) (2017) 799–806, https://doi.org/10.1038/nchembio.2389.

[56] J.-P. Vilardaga, F.G. Jean-Alphonse, T.J. Gardella, Endosomal generation of cAMP in GPCR signaling, Nat. Chem. Biol. 10 (9) (2014) 700–706.

[57] A. Godbole, S. Lyga, M.J. Lohse, D. Calebiro, Internalized TSH receptors en route to the TGN induce local Gs-protein signaling and gene transcription, Nat. Commun. 8 (2017) 443, https://doi.org/10.1038/s41467-017-00357-2.